19th INTERNATIONAL CONGRESS ON ACOUSTICS
MADRID, 2-7 SEPTEMBER 2007

MODELING RADIATION SYNTHESIS WITH SPHERICAL LOUDSPEAKER ARRAYS

PACS: 43.60.Fg

Franz Zotter, Robert Höldrich
Institute of Electronic Music and Acoustics, Graz, Austria
E-mail: zotter@iem.at, hoeldrich@iem.at

ABSTRACT

Spherical loudspeaker arrays are particularly suited for acoustic radiation synthesis in real or virtual reality environments. The spherical arrays in the scope of our paper basically consist of a rigid spherical body or platonic solid into which individually driven loudspeakers are mounted. Recently, there have been several publications describing the control of radiation patterns given specific array implementations (Warusfel [2][8], Kassakian [9], Behler [5][12], and Avizienis [11]). Our aim here is to model this kind of arrays analytically. For this purpose we use a model of the boundary conditions for the sound particle velocity imposed by the motion of the speakers. According to a suitable expansion of this problem into spherical base solutions (cf. Giron [1], Williams [3], Gumerov[10]) we presented in [13], we are able to describe the radiated sound field. In this paper, we extend our model with a description of the acoustic coupling between the loudspeakers due to the exterior sound field and the common enclosure volume. Finally, we verify the expressions emerging from this approach by comparing them to measurements of a hardware array.

SPHERICAL CAP MODEL

We model spherical loudspeaker arrays as a set of L spherical caps in a rigid spherical shell that may vibrate at their individual velocity (cf. [13], see also Meyer [4]). To keep the model simple, we postulate that a cap is a segment of a pulsating sphere with velocity $v^{(l)}$. Therefore, the radial velocity[1] is restricted to be equal at each point on the cap.

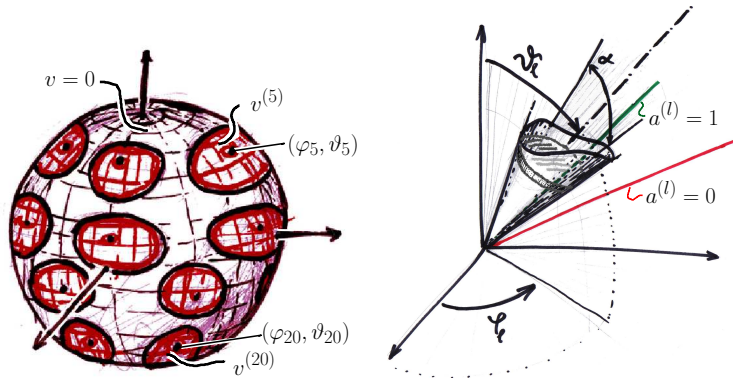

(a) The array model with individually vibrating spherical caps.

(b) The aperture of the l^{th} cap is 1 inside a cone with angle α opening towards (φ_l, ϑ_l), and 0 elsewhere.

Figure 1: Spherical cap model.

Fig. 1(a) shows a set of caps, in which the l^{th} spherical cap is centered around (φ_l, ϑ_l). Allowing for a finite thickness, we introduce r_i the inner, and r_o the outer radius of the shell sphere with $r_i < r_o$.

[1] Note that every quantity in this paper is described in the frequency domain. We skipped the frequency variable ω for better readability.

Cap Aperture Functions and Velocity Distribution
A cap membrane of our model can be described as an angular distribution which equals 1 inside, and 0 outside its respective region. Specifically, this cap region is enclosed by a cone of angle α with its apex at the origin $r = 0$, and its symmetry axis extending towards (φ_l, ϑ_l), see Fig. 1(b):

$$a^{(l)}(\varphi,\vartheta) \;=\; 1 - u\left\{\left\langle \begin{bmatrix}\cos(\varphi_l)\sin(\vartheta_l)\\ \sin(\varphi_l)\sin(\vartheta_l)\\ \cos(\vartheta_l)\end{bmatrix}, \begin{bmatrix}\cos(\varphi)\sin(\vartheta)\\ \sin(\varphi)\sin(\vartheta)\\ \cos(\vartheta)\end{bmatrix}\right\rangle - \cos\left(\frac{\alpha}{2}\right)\right\}. \tag{1}$$

The unit step function $u\{x\}$ in Eq. 1 equals 1 for positive x, and 0 otherwise. Its argument x is the scalar product $\cos(\theta) = \langle \vec{x}, \vec{y} \rangle$ describing the angle θ between the unit vectors $\|\vec{x}\| = \|\vec{y}\| = 1$.

Considering Eq. 1, we may define a surface velocity distribution for all the moving caps. This distribution is valid at the inner, as well as the outer surface of the shell, i.e. $r = r_i$, and $r = r_o$:

$$v(\varphi,\vartheta)|_{r_i,r_0} \;=\; \sum_{l=1}^{L} a^{(l)}(\varphi,\vartheta)\cdot v^{(l)}. \tag{2}$$

Note that Eq. 2 also characterizes the motionless parts of the shell ($v = 0$).

Spherical Harmonics Domain
In general, we may just as well express distributions $a(\varphi,\vartheta)$ on the sphere in terms of their spherical harmonics expansion coefficients A_{nm}, according to:

$$a(\varphi,\vartheta) \;=\; \sum_{nm=1}^{(N+1)^2} A_{nm}\cdot Y_{nm}(\varphi,\vartheta), \tag{3}$$

$$A_{nm} \;=\; \mathcal{SHT}\{a(\varphi,\vartheta)\} \;=\; \iint_{\mathbb{S}^2} a(\varphi,\vartheta)\cdot Y^*_{nm}(\varphi,\vartheta)\cdot d\Omega. \tag{4}$$

We use $nm = n^2 + n + 1 + m$ for linear indexing of the spherical harmonics $Y_{nm}(\varphi,\vartheta)$; N denotes the truncation number for the degree $n \le N$, i.e. $1 \le nm \le (N+1)^2$. Ideally, N should approach large numbers ($N \to \infty$). The interested reader can refer to Kostelec [7]. In particular, the transform of Eq. 1 yields (like in [13]):

$$A^{(l)}_{nm} \;=\; \mathcal{SHT}\left\{a^{(l)}(\varphi,\vartheta)\right\} \;=\; Y^*_{nm}(\varphi_l,\vartheta_l)\cdot 2\pi N_{nm}\int_{\cos\left(\frac{\alpha}{2}\right)}^{1} P_n[\cos(\vartheta)]\cdot d(\cos(\vartheta)), \tag{5}$$

where N_{nm} are the normalization constants, and $P_n(x)$ are the Legendre polynomials (cf. Williams [3], or Gumerov [10]).

Matrix/Vector Notation for Spherical Harmonics Expansions
Given the cap expansion coefficients $A^{(l)}_{nm}$ from Eq. 5, we are able to build an $(N+1)^2$ element vector $\vec{A}^{(l)}$. Furthermore, for a set of L different caps, we may build an $(N+1)^2 \times L$ matrix $\mathbf{A}$:

$$\mathbf{A} = \left[\vec{A}^{(1)},\ldots,\vec{A}^{(L)}\right], \qquad \vec{A}^{(l)} = \mathbf{vec_{SH}}\left\{A^{(l)}_{nm}\right\} := \begin{bmatrix} A^{(l)}_{0,\,0}\\ A^{(l)}_{1,-1}\\ \vdots\\ \left.\begin{matrix}A^{(l)}_{n,-n}\\ \vdots\\ A^{(l)}_{n,n}\end{matrix}\right\} 2n+1\\ \vdots\\ A^{(l)}_{N,N}\end{bmatrix}. \tag{6}$$

For expansions A_n depending on n only, the corresponding vector element A_n has to be repeated $2n+1$ times. Later in this text, we use the expression $\mathbf{diag_{SH}}\{A_n\}$, which is a diagonal matrix

containing this kind of vector:

$$\mathbf{diag_{SH}}\left\{A_n\right\} \quad := \quad \begin{bmatrix} A_0 & 0, & 0 & 0 & 0 & \dots & 0 \\ 0 & A_1 & 0 & 0 & 0 & \dots & 0 \\ 0 & 0 & A_1 & 0 & 0 & \dots & 0 \\ 0 & 0 & 0 & A_1 & 0 & \dots & 0 \\ 0 & 0 & 0 & 0 & A_2 & \dots & 0 \\ \vdots & \vdots & \vdots & \vdots & \vdots & \ddots & 0 \\ 0 & 0 & 0 & 0 & 0 & \dots & A_N \end{bmatrix}. \tag{7}$$

MECHANICAL AND ACOUSTICAL INTERACTIONS

Sound Field-Induced Cap Forces

Assume we are given a static model, in which every cap is motionless, i.e. $v^{(l)} = 0, \forall l = 1, \dots, L$. Introducing interior and exterior sound fields, we can determine the impact forces on the spherical caps of the array model, cf. Fig. 2(a). First of all, we introduce sound pressure distributions on

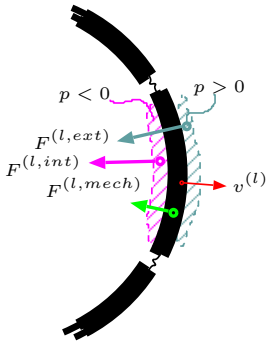

(a) Acoustical and mechanical forces on a spherical cap in radial direction.

(b) Laser Doppler vibrometry (LDV) measurements on an icosahedral loudspeaker array.

Figure 2: Acoustical forces and LDV measurement setup.

either side of the spherical shell, i.e. $p^{(ext)}\left(\varphi,\vartheta\right)|_{r_o}$ on the exterior, and $p^{(int)}\left(\varphi,\vartheta\right)|_{r_i}$ on the interior side. Integrating both sound pressures over the aperture $a^{(l)}\left(\varphi,\vartheta\right)$ of the l^{th} motionless cap yields the induced radial force $F^{(l)}$, cf. Fig. 2(a):

$$F^{(l)} \quad = \quad \iint_{\mathbb{S}^2} a^{(l)}\left(\varphi,\vartheta\right) \cdot \left[p^{(ext)}\left(\varphi,\vartheta\right)\Big|_{r_o} + p^{(int)}\left(\varphi,\vartheta\right)\Big|_{r_i} \right] \cdot d\Omega. \tag{8}$$

For the next step, we introduce the transforms, according to Eq. 4:

$$\Psi_{nm}^{(ext)}\Big|_{r_o} \; = \; \mathcal{SHT}\left\{ p^{(ext)}\left(\varphi,\vartheta\right)\Big|_{r_o} \right\}, \text{ and } \quad \Psi_{nm}^{(int)}\Big|_{r_i} \; = \; \mathcal{SHT}\left\{ p^{(int)}\left(\varphi,\vartheta\right)\Big|_{r_i} \right\}. \tag{9}$$

Inserting the spherical harmonics expansions Eq. 5 and Eq. 9 into the integral Eq. 8, we may exploit the orthonormality of the normalized spherical harmonics, cf. Gumerov [10]:

$$\begin{aligned} F^{(l)} \quad &= \quad \iint_{\mathbb{S}^2} \left[\sum_{nm'} A_{nm'}^{(l)} Y_{nm'}\left(\varphi,\vartheta\right) \right] \cdot \left[\sum_{nm} \left(\Psi_{nm}^{(ext)}\Big|_{r_o} + \Psi_{nm}^{(int)}\Big|_{r_i} \right) Y_{nm}\left(\varphi,\vartheta\right) \right] d\Omega, \\ &= \quad \sum_{nm} \sum_{nm'} A_{nm'}^{(l)} \left(\Psi_{nm}^{(ext)}\Big|_{r_o} + \Psi_{nm}^{(int)}\Big|_{r_i} \right) \cdot \underbrace{\iint_{\mathbb{S}^2} Y_{nm}\left(\varphi,\vartheta\right) Y_{nm'}\left(\varphi,\vartheta\right) d\Omega}_{=\delta[n-n']\delta[m+m']} \\ F^{(l)} \quad &= \quad \sum_{nm=1}^{(N+1)^2} A_{nm}^{*(l)} \cdot \left(\Psi_{nm}^{(ext)}\Big|_{r_o} + \Psi_{nm}^{(int)}\Big|_{r_i} \right). \end{aligned} \tag{10}$$

Note that changing the sign of m is equivalent to the complex conjugate, hence $A_{nm}^{*(l)} = A_{n,-m}^{(l)}$. Finally, using the matrix notation of Eq. 6, and its hermitian transpose $\mathbf{A^H}$ to re-write Eq. 10, we obtain a compact expression for the L impact forces:

$$\vec{F}^{(sf)} = \begin{bmatrix} F^{(1)} \\ F^{(2)} \\ \vdots \\ F^{(L)} \end{bmatrix} = \mathbf{A^H} \cdot \left(\vec{\Psi}^{(ext)}\Big|_{r_o} + \vec{\Psi}^{(int)}\Big|_{r_i} \right). \tag{11}$$

Cap Velocity-Induced Sound Field
Referring to the surface velocity in Eq. 2, we specify $\vec{\Upsilon}|_{ri,ro} = \mathbf{vec_{SH}}\{\mathcal{SHT}\{v(\varphi,\vartheta)\,|_{r_i,r_o}\}\}$:

$$\vec{\Upsilon}\Big|_{r_i,r_o} = \sum_{l=1}^{L} \vec{A}^{(l)} \cdot v^{(l)} = \mathbf{A} \cdot \begin{bmatrix} v^{(1)} \\ v^{(2)} \\ \vdots \\ v^{(L)} \end{bmatrix} = \mathbf{A} \cdot \vec{v}. \tag{12}$$

In the following lines, we use the spherical base solutions of the Helmholtz equation (cf. Giron [1], Williams [3], Gumerov [10]) to compute the exterior and interior sound field radiated by $\vec{\Upsilon}|_{r_i,r_o}$.

Exterior Sound Field $(r \geq r_o)$
Using the spherical Hankel functions[2] $h_n(kr)$, and $h'_n(kr)$, its derivative, as well as the surface velocity $\Upsilon_{nm}|_{r_o}$, we find a description of the exterior sound field (cf. Giron [1], Williams [3]):

$$\begin{aligned} \Psi_{nm}^{(ext)}(kr) &= i\rho_0 c \cdot \frac{h_n(kr)}{h'_n(kr_o)} \cdot \Upsilon_{nm}|_{r_o}, \\ \vec{\Psi}^{(ext)}(kr) &= i\rho_0 c \cdot \mathbf{diag_{SH}}\left\{ \frac{h_n(kr)}{h'_n(kr_o)} \right\} \cdot \vec{\Upsilon}\Big|_{r_o}, \\ &= i\rho_0 c \cdot \mathbf{diag_{SH}}\left\{ \frac{h_n(kr)}{h'_n(kr_o)} \right\} \cdot \mathbf{A} \cdot \vec{v}, \end{aligned} \tag{13}$$

where $i = \sqrt{-1}$, the air density is $\rho_0 = 1.2$, the speed of sound $c = 343\mathrm{m/s}$, the wave number $k = \omega/c$, and $\mathbf{diag_{SH}}\left\{\frac{h_n(kr)}{h'_n(kr_o)}\right\}$ following the definition in Eq. 7.

Interior Sound Field $(r \leq r_i)$
Similarly, but with the spherical Bessel functions $j_n(k_i r)$ and the inner surface velocity $\Upsilon_{nm}|_{r_i}$, we obtain the interior sound field (cf. Williams [3]) in its vectorial form:

$$\begin{aligned} \vec{\Psi}^{(int)}(r) &= i\rho_0 c_i \cdot \mathbf{diag_{SH}}\left\{ \frac{j_n(k_i r)}{j'_n(k_i r_i)} \right\} \cdot \vec{\Upsilon}\Big|_{r_i}, \\ &= i\rho_0 c_i \cdot \mathbf{diag_{SH}}\left\{ \frac{j_n(k_i r)}{j'_n(k_i r_i)} \right\} \cdot \mathbf{A} \cdot \vec{v}. \end{aligned} \tag{14}$$

Here, we chose a different notation c_i and k_i to account for the propagation properties of the enclosure medium. For an interior filled with damping wool these are $c_i = 0.93 \cdot c$ and $k_i = k/0.93$.

Acoustical Forces
Now, inserting the sound fields of the vibrating caps (Eq. 13 and Eq. 14) into the equation of the impact forces on the motionless caps (Eq. 11), we obtain the acoustical cap forces $\vec{F}^{(sf)}$:

$$\vec{F}^{(sf)} = i\rho_0 c \cdot \mathbf{A^H} \cdot \mathbf{diag_{SH}}\left\{ \left(\frac{c_i}{c} \frac{j_n(k_i r_i)}{j'_n(k_i r_i)} + \frac{h_n(kr_o)}{h'_n(kr_o)} \right) \right\} \cdot \mathbf{A} \cdot \vec{v}. \tag{15}$$

Note that this approach is based on the principle of linear superposition.

[2] We use $h_n(kr) = h_n^{(2)}(kr)$ to provide a causal solution to the Fourier expansion $e^{i\omega t}$.

Mechanical Forces
We require specific radial mechanical forces $\vec{F}^{(mech)}$ to induce the velocities $\vec{v}$ on the spherical caps. These two quantities interconnect via the mechanical impedances $\vec{z}$ of the membranes:

$$\vec{F}^{(mech)} = \mathbf{diag}\left\{\vec{z}\right\} \cdot \vec{v}. \tag{16}$$

EQUATION OF MOTION – SPHERICAL CAP MODEL

We set up the inhomogeneous equation of motion with the excitation force vector $\vec{F}^{(exc)}$ as:

$$\vec{F}^{(exc)} = \vec{F}^{(sf)} + \vec{F}^{(mech)}. \tag{17}$$

Inserting the acoustical and mechanical forces (Eq. 15 and Eq. 16), this yields:

$$\begin{aligned} \vec{F}^{(exc)} &= \left[i\rho_0 c \cdot \mathbf{A^H} \cdot \mathbf{diag_{SH}} \left\{ \left(\frac{c_i}{c} \frac{j_n\left(k_i r_i\right)}{j_n'\left(k_i r_i\right)} + \frac{h_n\left(k r_o\right)}{h_n'\left(k r_o\right)} \right) \right\} \cdot \mathbf{A} + \mathbf{diag}\left\{\vec{z}\right\} \right] \cdot \vec{v}, \\ \vec{F}^{(exc)} &= \mathbf{Z} \cdot \vec{v}. \end{aligned} \tag{18}$$

The expression in the brackets represents the composite impedance matrix $\mathbf{Z}$. Using its inverse $\mathbf{Y}$, the admittance matrix:

$$\vec{v} = \mathbf{Y} \cdot \vec{F}^{(exc)}, \tag{19}$$

$$\mathbf{Y} = \left[i\rho_0 c \cdot \mathbf{A^H} \cdot \mathbf{diag_{SH}} \left\{ \left(\frac{c_i}{c} \frac{j_n\left(k_i r_i\right)}{j_n'\left(k_i r_i\right)} + \frac{h_n\left(k r_o\right)}{h_n'\left(k r_o\right)} \right) \right\} \cdot \mathbf{A} + \mathbf{diag}\left\{\vec{z}\right\} \right]^{-1}, \tag{20}$$

we can choose an arbitrary excitation force vector $\vec{F}^{(exc)}$ and calculate the resulting velocity vector $\vec{v} = f\{\vec{F}^{(exc)}\}$. The strength of this expression becomes obvious if we assume $\vec{F}^{(exc)}$, so that only a single cap is actively excited. Eventually, the resulting vector $\vec{v}$ displays motion due to acoustic coupling, too.

Exterior Sound Field Synthesis Applying Excitation Forces
For an exterior sound field synthesis we may combine Eq. 19 with Eq. 13:

$$\vec{\Psi}^{(ext)}\left(kr\right) = i\rho_0 c \cdot \mathbf{diag_{SH}} \left\{ \frac{h_n\left(kr\right)}{h_n'\left(kr_o\right)} \right\} \cdot \mathbf{A} \cdot \mathbf{Y} \cdot \vec{F}^{(exc)}. \tag{21}$$

The excitation forces $\vec{F}^{(exc)}$ needed to achieve a specific target pattern at kr can be calculated from the inversion of the above matrix equation. Note that in real loudspeaker arrays these excitation forces $\vec{F}^{(exc)}$ are controlled electrically, e.g. with driving voltages $\vec{u}^{(exc)}$.

Design Example
In Fig. 3, we compare the magnitude responses of $\mathbf{Y}\left(\omega\right)$ with laser Doppler vibrometry (LDV) measurements from a real, electrically driven icosahedral array (Fig. 2(b)). Therefore we insert the appropriate model parameters r_i, r_o, k_i, and c_i into Eq. 20. For the mechanical impedances $\vec{z}$ of the caps, we use an RLC model with $z = R + i\omega M + S/(i\omega)$ of the membranes. Measurements with the delta mass method (cf. Dickason [6]) yield the missing parameters M, S, and R.

Due to the proportionality between the forces $\vec{F}^{(exc,l)}$ and the driving voltages $\vec{u}^{(exc,l)}$ on the speakers, the curves in Fig. 3 verify our cap model. Theoretical resonances at higher frequencies appear to be damped in the LDV measurements. Deviations of the geometry (platonic solid, speaker cones and magnets), as well as losses in the damping wool might be the reason for this behavior.

ACKNOWLEDGEMENTS
We gratefully thank the Zukunftsfonds Steiermark (Prj. 3027) for supporting our research, and Alois Sontacchi for his project management. Special thanks also go to Christian Jochum and Peter Reiner for the assembly of the icosahedral speaker and performing the measurements.

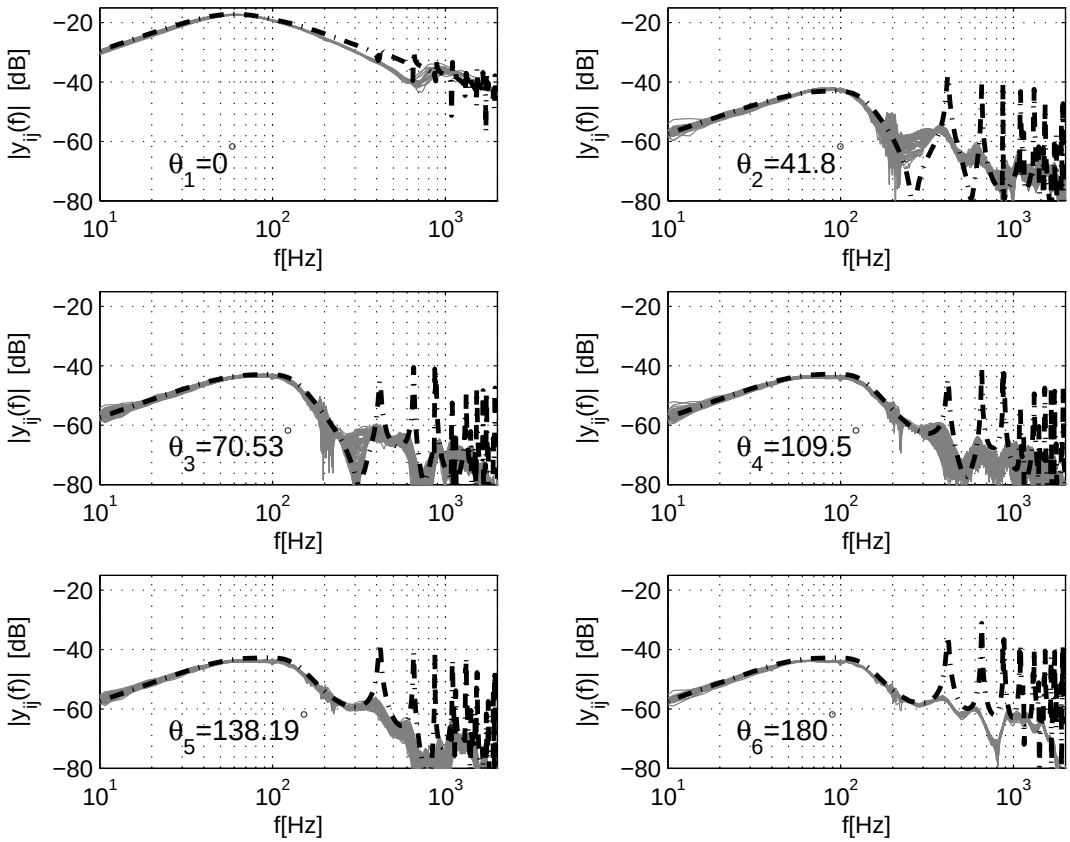

Figure 3: According to the icosahedral geometry of our test array, there are 6 types of admittance functions $y_{ij}(\omega) = \frac{v_i(\omega)}{F_j(\omega)}$, reflecting the distinct angular distance classes θ_ν of the array. The theoretical results of our cap model (black dashed) match the LDV measurement curves (thin gray) quite well.

References

[1] Giron, F.: Investigations about the Directivity of Sound Sources. EAA Fenestra, Bochum, 1996.

[2] O. Warusfel, P. Derogis and R. Caussé: Radiation Synthesis with Digitally Controlled Loudspeakers. 103rd AES-Convention, New York, 1997.

[3] Williams, E. G.: Fourier Acoustics. Academic Press, San Diego, 1999.

[4] P. S. Meyer and J. D. Meyer: Multi Acoustic Prediction Program (MAPP): Recent Results. Presented at the Institute of Acoustics (UK), 2000.

[5] G. Behler: Technique for the Derivation of Wide Band Room Impulse Response. Tecni Acustica, Madrid, 2000.

[6] Dickason, V.: Lautsprecherbau, Elektor-Verlag, 2001.

[7] P. J. Kostelec and D. N. Rockmore: FFTs on the Rotation Group. Tech. Report #: 03-11-060, Santa Fe Institute, New Mexico, 2003.

[8] O. Warusfel and N. Misdariis: Sound Source Radiation Synthesis: from Stage Performance to Domestic Rendering. 116th AES Convention, Berlin, 2004.

[9] P. Kassakian and D. Wessel: Characterization of Spherical Loudspeaker Arrays. 117th AES-Convention, San Francisco, 2004.

[10] N. A. Gumerov and R. Duraiswami: Fast Multipole Methods for the Helmholtz Equation in Three Dimensions. Elsevier, 2004.

[11] R. Avizienis, A. Freed, P. Kassakian, and D. Wessel: A Compact 120 Independent Element Spherical Loudspeaker Array with Programmable Radiation Patterns. 120th AES-Convention, Paris, 2006.

[12] G. Behler: How to Compare Concert Halls by Listening to Music. 4th ASA/ASJ joint meeting, Honolulu, 2006.

[13] F. Zotter, A. Sontacchi, and R. Höldrich: Modeling a Spherical Loudspeaker System as a Multipole Source. 33. DAGA, Stuttgart, 2007.